

International Journal of Modern Physics B
 © World Scientific Publishing Company

SATURATION OF THE INFRARED ABSORPTION BY CARBON DIOXIDE IN THE ATMOSPHERE

DIETER SCHILDKNECHT

*Fakultät für Physik, Universität Bielefeld
 D-33501 Bielefeld, Germany
 schild@physik.uni-bielefeld.de*

Received Day Month Year
 Revised Day Month Year

Based on new radiative transfer numerical evaluations, we reconsider an argument presented by Schack in 1972 that says that saturation of the absorption of infrared radiation by carbon dioxide in the atmosphere sets in as soon as the relative concentration of carbon dioxide exceeds a lower limit of approximately 300 ppm. We provide a concise brief and explicit representation of the greenhouse effect of the earth's atmosphere. We find an equilibrium climate sensitivity (temperature increase ΔT due to doubling of atmospheric CO_2 concentration) of $\Delta T \simeq 0.5^{\circ}C$. We elaborate on the consistency of these results on ΔT with results observationally obtained by satellite-based measurements of short-time radiation-flux versus surface-temperature changes.

Keywords: Greenhouse effect; Radiative transfer; Equilibrium climate.

1. Introduction

In view of the immense literature concerning the effect of an (anthropogenic) increase in the relative atmospheric carbon dioxide concentration on the earth's climate, it is appropriate to revive a simple argument on this subject presented by Schack¹ in 1972. The three-page article published in German in the journal of the German Physical Society, at that time called "Physikalische Blätter", appeared under the title "Der Einfluß des Kohlendioxid-Gehalts der Luft auf das Klima der Welt", i.e. "The influence of the carbon dioxide content of the air on the climate of the world". The author, Schack, an expert on heat transfer in combustion devices, in 1923 had discovered the role played by the interaction of infrared electromagnetic radiation with carbon dioxide, CO_2 , and water vapor, H_2O , in such devices².

The intensity of (monochromatic) radiation transversing an absorbing medium decreases exponentially with distance according to what is known as Lambert-Beer's law,

$$I(z) = I(z=0)e^{-\kappa z}. \quad (1.1)$$

Independently of the numerical value of the absorption constant κ in (1.1), for sufficiently large distance, z , the limit of "complete absorption", or zero intensity

2 *Dieter Schildknecht*

of the outgoing radiation, $I(z \rightarrow \infty) \rightarrow 0$, is reached. For finite values of the exponent $-\kappa z$ in (1.1), the numerical value of the κ determines the distance, $z_\epsilon(\kappa)$, for “approximate saturation”, $\exp(-\kappa z_\epsilon(\kappa)) = \epsilon \ll 1$, or equivalently, “almost full absorption”,

$$\frac{I(z=0) - I(z=z_\epsilon(\kappa))}{I(z=0)} = 1 - \frac{I(z=z_\epsilon(\kappa))}{I(z=0)} = 1 - \epsilon. \quad (1.2)$$

In the case of CO_2 in air, the wide band absorption constant κ for the infrared electromagnetic radiation depends on the concentration, or the partial pressure, of the CO_2 , and a natural question concerns the magnitude of the CO_2 concentration that leads to approximate saturation within the troposphere of the earth.

In his 1972 article¹, Schack points out that for a concentration of 0.03 % carbon dioxide in air, approximate saturation is reached within a distance of approximately the magnitude of the height of the troposphere. The absorption reaches values close to 100 % for a realistic CO_2 content of 0.03 %, it is concluded¹ that any further increase of (anthropogenic) CO_2 cannot lead to an appreciably stronger absorption of radiation, and consequently cannot affect the earth’s climate.

It will be useful to elaborate on the argument given by Schack in detail, in order to explicitly display the simplicity and generality of the underlying concepts that lead to a parameter-free prediction of the absorption of infrared radiation by CO_2 .

Adopting Planck’s radiation law for a temperature at the surface of the earth, chosen as $T = 293K$ by Schack, and taking into account the well-known absorption spectrum of the CO_2 molecule, one finds that the radiation of wave lengths λ_{CO_2} in the interval $13 \mu m \leq \lambda_{CO_2} \leq 17.6 \mu m$ is relevant for the absorption by CO_2 . The total absorption due to CO_2 in the atmosphere is determined by the total mass of CO_2 that is transversed by a beam of infrared radiation on its path from the surface at $z = 0$ to the upper end of the atmosphere, or $z \rightarrow \infty$.

In the gravitational field of the earth, the pressure, p , of a gas decreases with increasing altitude, z , according to $dp = -\rho g dz$, where ρ denotes the density of the gas and g the acceleration due to gravity. For an ideal gas of temperature T , we have $p = \rho RT/M$, or $\rho = pM/RT$, with R being the gas constant, T denoting the absolute temperature and M the molecular weight of the gas. The total mass per unit area transversed by a beam of infrared radiation on its path through the atmosphere is determined by an integration over the density $\rho(p, T)$ from the surface to the upper end of the troposphere. The result of the integration may be represented in terms of an effective altitude z_0 of a fictitious atmosphere of homogeneous constant pressure p_0 , constant temperature T and constant density ρ . The value of z_0 (obviously) depends on whether the atmosphere is treated isothermally, or rather more realistically, is described adiabatically.

Adopting $T = \text{const}$, the decrease of pressure with increasing altitude becomes equal to

$$p(z) = p_0 \exp\left(-\frac{Mg}{RT}z\right), \quad (1.3)$$

which is the well-known barometric formula. The density $\rho = \rho(z)$ decreases accordingly as

$$\rho(z) = \frac{M}{RT} p_0 \exp\left(-\frac{z}{z_0}\right) \equiv \rho_0 \exp\left(-\frac{z}{z_0}\right), \quad (1.4)$$

where

$$z_0 = \frac{RT}{Mg} \quad (1.5)$$

denotes the scale-height of the atmosphere, the height of a fictitious atmosphere of homogeneous pressure p_0 , temperature T and density ρ_0 , and a mass per unit area, M_0 , obtained from (1.4),

$$M_0 \equiv \int_0^\infty \rho(z) dz = \rho_0 z_0 = \frac{M p_0}{RT} z_0. \quad (1.6)$$

The determination of the absorption of the atmosphere is accordingly reduced to the evaluation of the absorption by a gas pipe of length z_0 from (1.5) homogeneously filled with air, and with CO_2 of partial pressure $p_0 \equiv p_{CO_2}$, at a total pressure of 1 atm at temperature $T = 293 K$.

For the realistic case of an adiabatically treated atmosphere relation (1.6) remains valid with an appropriately chosen value of z_0 different from (1.5). In our approach of Section 2 the value of z_0 will be determined from the altitude dependence of the absorption of infrared radiation for given lapse rate in the atmosphere.

The absorption due to (1.1), upon introducing the dependence on the CO_2 concentration via the partial pressure p_{CO_2} , becomes

$$A(p_{CO_2}, z_0) = 1 - \exp(-ap_{CO_2} z_0), \quad (1.7)$$

where the coefficient a must be determined from the known absorption spectrum of CO_2 . Since the absorption cross section of CO_2 depends on the wave length of the radiation being absorbed, the absorption constant a in (1.7), obtained by summation over a spectrum of a large number of spectral lines, actually develops a dependence on the partial pressure p_{CO_2} .

Table 1. The results given in the first four horizontal lines are taken from ref. ¹, the results in the last line are computed using (1.7).

CO_2 [%]	0.03 %	0.06 %	$\Delta_{2 \times CO_2}$ [%]	$\Delta_{2 \times CO_2} [Wm^{-2}]$
$p_{CO_2} z_0 [atm \times m]$	2.1	4.2		
A [%]	98.5 %	99.3 %	0.8 %	0.70
1 - A [%]	1.5 %	0.7 %		
$a [(atm \times m)^{-1}]$	2.0	1.73		

In his article¹, addressing the question on the effect of an increase of the CO_2 concentration on the climate on earth, Schack compares the absorption due to CO_2 , by a CO_2 -air pipe as mentioned, for a partial pressure corresponding to a realistic

value of 300 ppm = 0.03 % with the absorption due to an enhanced value taken as 600 ppm = 0.06 % ^a, respectively corresponding to $p_{CO_2} = 3 \times 10^{-4}$ atm and $p_{CO_2} = 6 \times 10^{-4}$ atm at $T = 293$ K and a total pressure of 1 atm of the atmosphere. Adopting $z_0 = 7000$ m for the equivalent height of the troposphere, for the absorption, A [%], and the increase of absorption, $\Delta_{2 \times CO_2}$, Schack obtains the results that are given in Table 1.

Saturation of infrared radiation by the realistic CO_2 content of the atmosphere of 0.03 % being reached within approximately 1 % according to Table 1, any further increase of the CO_2 content does not substantially increase the absorption of radiation, and accordingly does not affect¹ the climate on earth.

The results on $\Delta_{2 \times CO_2}$ [%] in Table 1 refer to the radiation in the CO_2 band of $13 \mu m \lesssim \lambda_{CO_2} \lesssim 17.6 \mu m$ ($568 \text{ cm}^{-1} \lesssim 1/\lambda_{CO_2} \lesssim 769 \text{ cm}^{-1}$). With the assumption of a black-body radiation at $T = 293 \text{ K}$, the input radiation in the CO_2 band amounts to 87 W/m^2 . The additional absorption due to CO_2 doubling is given by $\Delta_{2 \times CO_2} \times 87 \text{ W/m}^2 = 0.8 \times 10^{-2} \times 87 \text{ W/m}^2 = 0.70 \text{ W/m}^2$, as listed in Table 1. This increase of the absorption of infrared radiation in the atmosphere is indeed negligible in comparison with the equilibrium value of the total outgoing long-wave infrared radiation (LWIR) at the top of the atmosphere (TOA) given by $S_0 = 239 \text{ W/m}^2$. ^b

2. Absorption of Infrared Radiation: CO_2 -Air Pipe versus Atmosphere

Using presently available detailed data on the spectral absorption lines of CO_2 , compare⁵, the absorption coefficient^c a and the resulting absorption by a CO_2 -air pipe, defined before, can be reliably predicted. In this Section, we compare the results on absorption by a CO_2 -air pipe at fixed temperature and pressure, as a function of the length of the CO_2 -air pipe, with the absorption by an adiabatically treated atmosphere. The results to be presented are due to a recent evaluation by Clark⁷ for the $^{12}\text{C } ^{16}\text{O}_2$ molecule only, with linestrengths $> 10^{-23}$. We refer to Appendix A for further details.

The results⁷ for the absorption of a CO_2 -air pipe for the spectral range of $13 \mu m \lesssim \lambda_{CO_2} \lesssim 17.6 \mu m$ (568 cm^{-1} to 769 cm^{-1}), as a function of selected values of the path length (pipe length) and the relevant CO_2 concentrations of 0.03 % and 0.06 % are shown in Table 2. The pipe is assumed to have constant temperature, $T = 293 \text{ K}$, and a total pressure of $p = 1 \text{ atm}$. The input black-body infrared radiation at $T = 293 \text{ K}$ is accordingly given by 87 W/m^2 . The results in Table 2

^a A realistic value for the increase of the CO_2 concentration per year is 2 ppm/year, e.g.³, implying 150 years for the doubling of a CO_2 concentration of 300 ppm.

^bThe known empirical value of the sun radiation of 1365 W/m^2 with an albedo of 0.3 yields 956 W/m^2 absorption. Dividing by 4 to take into account the surface of the earth yields the average value of the radiation from the sun to be balanced by the outgoing average LWIR of $S_0 = 239 \text{ W/m}^2$. ⁴ A 1 % decrease of the albedo to become $\epsilon = 0.297$ yields $S_0 = 240 \text{ W/m}^2$ to be used subsequently.

^cCompare e.g. ref.⁶ for a recent evaluation of absorption coefficients

Table 2. CO_2 -air pipe absorption A and increase $\Delta_{2\times CO_2}$ for selected path lengths and CO_2 concentrations for the spectral range 568 to 769 cm^{-1} (input black-body radiation 87 Wm^{-2}) and $T = 293K$, $p = 1atm$. Compare Appendix A Table A2.

	A	A		
	300 ppm	600 ppm	$\Delta_{2\times CO_2}$ [%]	$\Delta_{2\times CO_2}[Wm^{-2}]$
1 km	0.63	0.71	8 %	7.00
2 km	0.71	0.78	7 %	6.09
3 km	0.75	0.82	7 %	6.09
5 km	0.81	0.87	6 %	5.22
7 km	0.84	0.89	5 %	4.35

Table 3. Same as Table 2, but for 600 cm^{-1} to 750 cm^{-1} spectral range (input black-body radiation 65 Wm^{-2}). Compare Appendix A Table A3.

	A	A		
	300 ppm	600 ppm	$\Delta_{2\times CO_2}$ [%]	$\Delta_{2\times CO_2}[Wm^{-2}]$
1 km	0.79	0.87	8 %	5.20
2 km	0.87	0.93	6 %	3.90
3 km	0.91	0.96	5 %	3.25
5 km	0.95	0.98	3 %	1.95
7 km	0.97	0.99	2 %	1.30

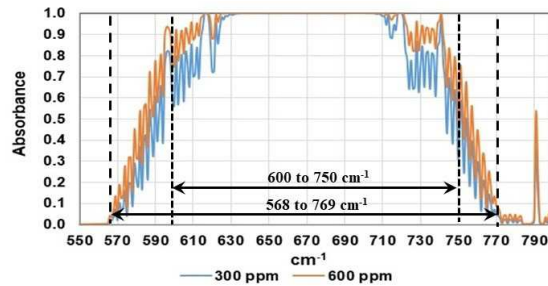


Fig. 1. The absorbance of 0.03 % and 0.06 % concentrations of CO_2 in dry air at 293 K for a 3 km CO_2 -air pipe. The spectral ranges of 568 to 769 cm^{-1} and 600 to 750 cm^{-1} used in the absorption band calculations are indicated. The calculation ⁷ was performed at a spectral resolution of 0.01 cm^{-1} , but the data are plotted at 1 cm^{-1} .

explicitly demonstrate the expected increase of the absorption A with increasing length of the pipe (path length), as well as the decrease of the relative absorption for CO_2 doubling, $\Delta_{2\times CO_2}$ [%]. The result of $\Delta_{2\times CO_2} = 5\%$ at the pipe length of 7 km is considerably larger than the 1972 result of $\Delta_{2\times CO_2} = 0.8\%$ given in Table 1.

In Table 3, for illustration, we show the effect of restricting the spectral range of the input black-body radiation to the spectral range of 600 cm^{-1} to 750 cm^{-1} (total black-body radiation 65 Wm^{-2}). Comparing the results in Table 3 with the ones in Table 2, we notice the more rapid approach to a (larger) asymptotic absorption limit with increasing path length of the infrared radiation. This is a consequence

of the change of absorbance as a function of the spectral wave length taken into account.

In Fig. 1, we show the calculated spectrum of the absorbance for the case of a path length of 3 km and a CO_2 concentration of 0.03% and 0.06%. The spectral ranges corresponding to Tables 2 and 3 are indicated in Fig. 1.

Turning from fixed temperature T in the CO_2 -air pipe to decreasing T and pressure p in the atmosphere, we proceed in two steps. In a first step, modelling a dry atmosphere, we consider the effect of CO_2 (at concentrations of 0.03% and 0.06%), and in a second step, we add water vapor of fixed relative humidity (RH) chosen as $RH = 85\%$.

Table 4. Altitude dependence of the infrared absorption A by the atmosphere for selected altitudes and CO_2 concentrations for the 568 to 769 cm^{-1} spectral range (input black-body radiation $87 Wm^{-2}$). Surface temperature and surface pressure are $T = 293 K$ and $p = 1 atm$, and the lapse rate adopted for the atmosphere is given by $-6.5 ^\circ C km^{-1}$. Compare Appendix A Table A4.

	A 300 ppm	A 600 ppm	$\Delta_{2 \times CO_2}$ [%]	$\Delta_{2 \times CO_2} [Wm^{-2}]$
Atm 5 km	0.74	0.81	7 %	6.09
Atm 9 km	0.76	0.83	7 %	6.09
Atm 11 km	0.76	0.83	7 %	6.09

Table 5. Same as Table 4, but for a 600 to 750 cm^{-1} spectral range (input black body emission $65 Wm^{-2}$). Compare Appendix A Table A4.

	A 300 ppm	A 600 ppm	$\Delta_{2 \times CO_2}$ [%]	$\Delta_{2 \times CO_2} [Wm^{-2}]$
Atm 5 km	0.90	0.95	5 %	3.25
Atm 9 km	0.91	0.96	5 %	3.25
Atm 11 km	0.91	0.96	5 %	3.25

In Table 4, we show the results for the absorption A of the atmosphere at several selected altitudes for a CO_2 content of 0.03% and 0.06%. The spectral range of the LWIR of 568 cm^{-1} to 769 cm^{-1} is identical to the spectral range employed for the results in Table 2. The evaluation of the absorption was carried out for a surface temperature of $T = 293 K$ and a surface pressure $p = 1 atm$, and a realistic moist adiabatic lapse rate increasing with altitude, and an average value of $-6.5 ^\circ C km^{-1}$ was employed (compare Appendix A, Fig. A6). The absorption spectrum at 0.01 cm^{-1} resolution was calculated using a spatial resolution of 100 m. The absorption spectrum for each 100 m level was calculated using the pressure and temperature for that level derived from the lapse rate. The results in Table 4 show a rapid convergence to an approximately constant, quasi-asymptotic behavior of the absorption A that is reached above an altitude of approximately 5 km. By

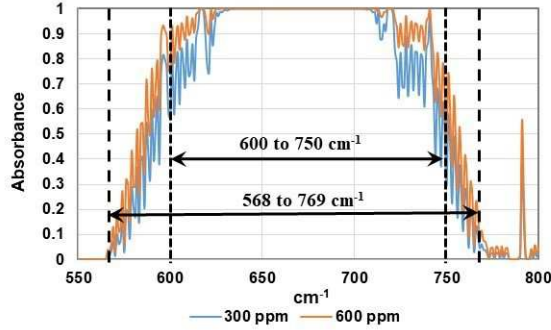


Fig. 2. The absorbance of 0.03 % and 0.06 % concentrations of CO_2 in a dry atmosphere for a vertical path length from the surface to 7 km altitude. The surface temperature is 293 K. The lapse rate is -6.5 K km^{-1} and the spatial resolution is 100 m. The calculation ⁷ was performed at a spectral resolution of 0.01 cm^{-1} , but the data are plotted at 1 cm^{-1} resolution.

comparison of the results in Table 4 with the ones in Table 2, we conclude that a CO_2 -air pipe for a chosen length of 2 to 3 km represents the absorption of the atmosphere that reaches a quasi-asymptotic limit at altitudes of about 5 km. The values of the absorption and the increase of the absorption under CO_2 doubling of $\Delta_{2 \times CO_2} = 7\%$ corresponding to 6 W m^{-2} in Tables 2 and 4 are in agreement with each other. Similar conclusions are drawn from the comparison of the results for the restricted spectral range in Tables 3 and 5 with each other.

In Fig. 2, we show the absorption of the surface emission at 293 K of 300 and 600 ppm of CO_2 for the dry atmosphere looking downwards from a height of 7 km. The total spectral range is from 550 to 800 cm^{-1} and the spectral intervals are indicated. These are the same as for Fig. 1. The spectral resolution of the calculation was 0.01 cm^{-1} with a spatial resolution of 100 m. The spectral resolution of the plot however, is 1 cm^{-1} . This spectrum includes the effects of the decrease in temperature and pressure with altitude as shown in Appendix A, Fig. A6. In this case most of the absorption occurs near the surface and the value of the total absorption tends towards an asymptotic value as the altitude increases. This is shown in Appendix A, Fig. A4.

The results explicitly demonstrate that the CO_2 -air pipe of path length of approximately 3 km represents the absorption in the atmosphere of a quasi-asymptotic altitude reached at 5 km.

The important role of water vapor – semi-quantitatively discussed in ref.¹ – is illustrated by comparing the results in Tables 4 and 5 with the results presented in Tables 6 and 7. The results in Tables 6 and 7, in addition to CO_2 , take into account water vapor with relative humidity (RH) of $\text{RH} = 85\%$. The presence of water vapor drastically reduces^d the effect of doubling the CO_2 concentration from 6.09 W m^{-2}

^dNote that (obviously) the presence of water vapor increases the absorption of radiation. The presence of water vapor, however, decreases the effect of an increase of the CO_2 concentration.

Table 6. Same as Table 4, but including the absorption by water vapor of relative humidity (RH) of 85 %. Compare Appendix A, Table A5.

	A 300 ppm	A 600 ppm	$\Delta_{2\times CO_2}$ [%]	$\Delta_{2\times CO_2}$ [Wm^{-2}]
Atm 5 km 85 RH	0.89	0.92	3 %	2.6
Atm 9 km 85 RH	0.90	0.93	3 %	2.6
Atm 11 km 85 RH	0.90	0.93	3 %	2.6

Table 7. Same as Table 5, but including the absorption by water vapor of relative humidity (RH) of 85 %. Compare Appendix A, Table A5.

	A 300 ppm	A 600 ppm	$\Delta_{2\times CO_2}$ [%]	$\Delta_{2\times CO_2}$ [Wm^{-2}]
Atm 5 km 85 RH	0.94	0.97	3 %	2.0
Atm 9 km 85 RH	0.95	0.98	3 %	2.0
Atm 11 km 85 RH	0.95	0.98	3 %	2.0

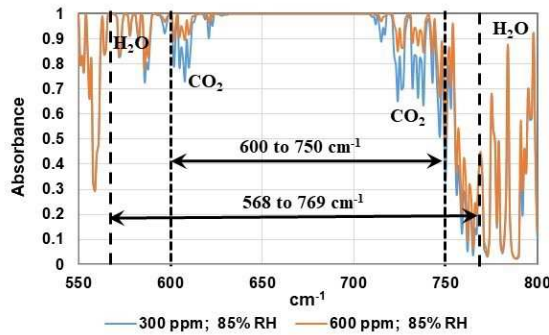


Fig. 3. The absorbance of 0.03 % and 0.06 % concentrations of CO_2 in a moist atmosphere for a vertical path length from the surface to 7 km altitude. The surface temperature is 293 K. The relative humidity at the surface is 85 %. The lapse rate is -6.5 K km^{-1} up to the saturation level the spatial resolution is 100 m. The calculation ⁷ was performed at a spectral resolution of 0.01 cm^{-1} , but the data are plotted at 1 cm^{-1} resolution.

to about 2.6 W m^{-2} for the infrared spectral range of $568 \text{ to } 769 \text{ cm}^{-1}$. A similar effect is seen by comparing the results in Tables 5 and 7 with each other.

For comparison with Fig. 2, in Fig. 3, we show the absorption spectrum in the atmosphere for the presence of water vapor in addition to carbon dioxide.

Compare ref.¹ for a semi-quantitative discussion.

In summarizing this Section we conclude that a CO_2 -air pipe of path length of 2 to 3 km represents the effect of the CO_2 increase in the atmosphere which has reached its quasi-asymptotic saturation limit at an altitude of approximately 5 km. Inclusion of water vapor drastically reduces the effect on the absorption of a rise of the CO_2 concentration from 0.03% to 0.06% from about $6W m^{-2}$ to $3W m^{-2}$. The value of $3W m^{-2}$ additional absorption corresponding to $3/418 \simeq 0.7\%$ of the total outgoing radiation at the surface of the earth, we conclude that the doubling of the CO_2 concentration for the relevant time scale of about a century is a fairly negligible one. Even though the increase of absorption of $\Delta_{2 \times CO_2} \simeq 3W m^{-2}$ is considerably larger than the 1972 value of $\Delta_{2 \times CO_2} \simeq 1W m^{-2}$, the main conclusion from ref.¹ remains valid.

3. CO_2 Doubling and Surface Temperature

In Section 2, we concluded that the absorption of infrared radiation from the CO_2 band in the atmosphere becomes (approximately) independent of the altitude for altitudes larger than about 5 km; the absorption reaches a quasi-asymptotic saturation limit at an altitude of about 5 km. The magnitude of the quasi-asymptotic absorption agrees with the absorption of a CO_2 -air pipe at constant temperature, $T = 293K$, and constant pressure, $p = 1atm$, and length of about 2 to 3 km.

The evaluation⁷, compare Appendix A for details, of the absorption by the atmosphere is based on the known spectroscopic properties of the absorbing gases, H_2O , CO_2 , and the empirically known average lapse rate of the atmosphere of about $-6.5K km^{-1}$. The absorption reaches an approximately constant value at an altitude of 6 km. At and beyond that height, a constant value of infrared radiation is freely emitted to space. At this height, the atmosphere provides a “free window” (compare Appendix B) for the emittance of infrared radiation at temperature $T_{TOA} = (293 - 6 \times 6.5)K = 254K \simeq 255K$. The outgoing intensity is given by $S_{space} = S(T)|_{T=255K} = \sigma T^4|_{T=255} = 240 W m^{-2}$.

The approximate stability of the climate on earth, a necessary condition for life on earth, requires equilibrium of the outgoing infrared radiation, predicted by $S_{space} = S(T)|_{T=255K}$, with the effective radiation provided by the sun. The effective radiation by the sun amounts^e to $S_0 = 240W m^{-2}$. The agreement of the above parameter-free prediction of the radiative transfer calculation, with the effective radiation from the sun,

$$S_{space} = S(T)|_{T=255K} = S_0, \quad (3.1)$$

provides a non-trivial support of the radiative-transfer calculation based on the empirical lapse rate of $6.5K m^{-2}$. Indeed, the radiative-transfer analysis explains the approximate stability of the climate on earth.

For a concise representation of the radiative “greenhouse effect” in terms of the radiation from the sun, S_0 , and the earth’s LWIR within as well as outside

^eCompare footnote 3

the “atmospheric window”, as quantified by S_W , and the fractional transmittance, $f' \ll 1$, respectively, compare Appendix B.

We turn to the effect of CO_2 doubling on the surface temperature. We assume the existence of radiative equilibrium of the emitted black-body LWIR, given by $S(T)$, for any given CO_2 content (within the presently discussed limits). Absorption under doubling of the CO_2 concentration, $\Delta_{2 \times CO_2}$, for compensation requires increase of radiation $S(T) \rightarrow S(T) + \Delta S$, i.e.

$$S(T) + \Delta S = S(T + \Delta T) = S(T) + \left. \frac{dS}{dT} \right|_T \Delta T, \quad (3.2)$$

where $\Delta S \equiv \Delta_{2 \times CO_2}$ and T denotes the surface temperature, chosen as $T = 293K$ in our treatment. Note that the detailed mechanism occurring in the atmosphere leading to the required increase of $\Delta S = \Delta_{2 \times CO_2}$ need not be specified. According to (3.2), the temperature has to rise by

$$\Delta T = \frac{\Delta_{2 \times CO_2}}{\left(\frac{dS}{dT} \right)_T} = \frac{T \Delta_{2 \times CO_2}}{4S(T)}, \quad (3.3)$$

where $S(T) \sim T^4$ for a Planck radiator is used in the last step. Relation (3.3) specifies the rise of the surface temperature connected with restoration of equilibrium at the end of a CO_2 -air pipe, or equivalently, at the altitude of the atmosphere where the quasi-asymptotic limit of the absorption has been reached. Inserting $T = 293K$, and $S(T = 293K) = 418Wm^{-2}$, as well as $\Delta_{2 \times CO_2} = 6.09W m^{-2}$ from Tables 2 and 4 into (3.3), we obtain an increase of surface temperature of $\Delta T = 1.07 K$, compare Table 8. Insertion of $\Delta_{2 \times CO_2} = 2.6W m^{-2}$ from Table 6 into (3.3) shows the strong effect of water vapor of $RH = 85\%$. The strong absorption due to H_2O diminishes the surface-temperature change to $\Delta T = 0.46K$ for the assumed increase of the CO_2 concentration from 0.03% to 0.06%.

Table 8. The increase of surface temperature compensating infrared absorption by CO_2 and by $CO_2 + H_2O$ with $RH = 85\%$

	$\Delta_{2 \times CO_2} [Wm^{-2}]$	$\Delta T [K]$
3 km CO_2 -air pipe	6.09	1.07
9 km Atmosphere		
9 km Atmosphere $RH = 85\%$	2.6	0.46

4. Radiative Absorbance under Change of Atmospheric Conditions.

A very elaborate radiative transfer calculation, recently presented by Harde¹⁰, within a two-layer climate model, explores^f the infrared absorbance by CO_2 under

^fCompare refs.^{8,9} for alternative dynamical climate models.

a variety of atmospheric conditions, such as surface temperature, humidity, clouds etc. Results¹⁰ on the radiative absorbance for CO_2 contents of 380 ppm and 760 ppm, under variation of the atmospheric conditions, are shown in Table 9.

Table 9. The first three columns quote the results obtained by Harde¹⁰ for the absorbance of infrared radiation for CO_2 concentrations of 0.038 % and 0.076 % , and the increase $\Delta_{2\times CO_2}$ [%], under different atmospheric conditions, such as surface temperature, humidity, clouds etc. In the remaining four columns, we present the associated increase, $\Delta_{2\times CO_2}$ [Wm^{-2}], and the surface temperature increase, ΔT , and the averages $\overline{\Delta_{2\times CO_2}}$ and $\overline{\Delta T}$.

0.038 %	0.076 %	$\Delta_{2\times CO_2}$ [%]	$\Delta_{2\times CO_2}$ [Wm^{-2}]	ΔT [K]	$\overline{\Delta_{2\times CO_2}}$ [Wm^{-2}]	$\overline{\Delta T}$ [K]
82.57 %	83.84 %	1.27 %	5.03	0.92		
82.57 %	83.31 %	0.74 %	2.93	0.53	3.45	0.63
89.77 %	90.48 %	0.71 %	2.81	0.51		
81.55 %	82.05 %	0.50 %	1.98	0.36		
84.08 %	85.22 %	1.14 %	4.51	0.82		

We note that the results for the absorbance in Table 9 give the absorption due to CO_2 doubling as a fraction of the total LWIR of $S(T) = 396 Wm^{-2}$ at $T = 289 K$ employed by Harde, compared to Tables 2, 3 through 6, 7 that give the results for the increase of absorbance from CO_2 doubling as a fraction of the radiation in the CO_2 band. For a detailed discussion, we refer to ref.¹⁰.

In the context of the present discussion, the essential and important point of the results in Table 9 is the approximate independence of the absorption due to CO_2 doubling, $\Delta_{2\times CO_2} \cong 1\%$, from the various atmospheric conditions evaluated. Compare the results for $\Delta_{2\times CO_2}$ in column 3 of Table 9. The spread of the results for ΔT in column 5 of Table 9 between $\Delta T = 0.36K$ and $\Delta T = 0.92K$, and the average value of $\overline{\Delta T} = 0.63K$, are consistent with the result from our straight-forward evaluation of $\Delta T = 0.46K$ in Table 8.

The consistency or approximate agreement of our result of $\Delta T = 0.46 \simeq 0.5K$ in Table 8, and the result of $\overline{\Delta T} \cong 0.6K$ in Table 9 requires additional comments. The agreement strengthens the validity of our result based on what may be called a single-layer (surface) model, particularly evident from the equivalence of the atmosphere and the CO_2 -air pipe running at surface temperature and surface pressure. On the other hand, we conclude that much of the involved details of various flux terms of a two-layer model can apparently be summarized by our simple radiative equilibrium assumption for ΔT in (3.3). For a supplementary discussion on ΔT we refer to the last part of Appendix B.

5. On Observationally Testing the Radiative Transfer Results

The experimental tests of predictions on the climate sensitivity in general require decadal or even centennial time scales. In pioneering papers by Lindzen and Choi¹⁴ it was pointed out that data on fluctuations of the earth's (sea-)surface temperature at short time scales, once combined with satellite-based radiation-flux measurements^{15,16}, can be employed to gain important empirical information on the earth's climate sensitivity. In response to immediate reactions in the literature^{17,18,19} on their results¹⁴, an additional more expanded and refined investigation was presented by Lindzen and Choi²⁰. Compare also ref.²¹ for a more recent related investigation.

In what follows, we shall point out that the results from combining the data of sea-surface temperature fluctuations with data on radiation-flux intensities from the ERBE¹⁵ and CERES¹⁶ experiments empirically support our results on ΔT from the radiative-transfer analysis given in Sections 2 to 4. We restrict ourselves to elaborating on the basic underlying assumptions and the final conclusion from them. Entering a discussion on the technical details involved in the analysis of the experimental data is far beyond our expertise.

In the radiative-transfer calculations in Sections 2 and 3, we proceeded in two distinct steps. In a first step, we treated a dry atmosphere (zero humidity), in the second step the realistic case of non-zero humidity was investigated. It will be useful to introduce a notation referring to these two cases explicitly. Specializing (3.3) to the cases of zero and non-zero humidity, we define

$$\Delta T^{(0)} = \frac{\Delta_{2 \times CO_2}^{(0)}}{\left(\frac{dS}{dT}\right)_T} \equiv G(T) \Delta_{2 \times CO_2}^{(0)}, \quad (5.1)$$

and

$$\Delta T^{(H)} = \frac{\Delta_{2 \times CO_2}^{(H)}}{\left(\frac{dS}{dT}\right)_T} \equiv G(T) \Delta_{2 \times CO_2}^{(H)}, \quad (5.2)$$

related to zero and non-zero humidity, respectively. We recall the numerical values of $G = G(T = 293K) = \frac{293}{4 \times 418} = 0.175 KW^{-1}m^2$, as well as $\Delta_{2 \times CO_2}^{(0)} = 6.09 Wm^{-2}$ and $\Delta_{2 \times CO_2}^{(H)} = 2.6 Wm^{-2}$ given in Section 3.

Identically rewriting $\Delta T^{(H)}$ as

$$\Delta T^{(H)} = \Delta T^{(0)} + \Delta T^{(H)} - \Delta T^{(0)} \equiv \Delta T^{(0)} + f \Delta T^{(H)}, \quad (5.3)$$

we find that the commonly employed so-called feedback factor f , with (5.1) and (5.2), is given by

$$f = 1 - \frac{\Delta T^{(0)}}{\Delta T^{(H)}} = 1 - \frac{\Delta_{2 \times CO_2}^{(0)}}{\Delta_{2 \times CO_2}^{(H)}}, \quad (5.4)$$

or equivalently,

$$\Delta T^{(H)} = \frac{\Delta T^{(0)}}{1 - f}. \quad (5.5)$$

Numerically, from (5.4) and Table 8, we find the value of f from the radiative-transfer calculation, henceforth called the theoretical value of $f = f_{th}$, to be given by

$$f_{th} = 1 - \frac{6.09}{2.6} = -1.34. \quad (5.6)$$

The negative feedback factor, upon insertion into (5.5), thus identically reproduces

$$\Delta T^{(H)} = \frac{\Delta T^{(0)}}{2.34} = \frac{1.07}{2.34} = 0.46K < 1.07K \quad (5.7)$$

from Table 8.

Replacing $\Delta_{2 \times CO_2}^{(H)}$ in (5.4) by $\Delta T^{(H)}$, by employing (5.2), the factor f may be rewritten as

$$f = 1 - G(T) \frac{\Delta_{2 \times CO_2}^{(0)}}{\Delta T^{(H)}}. \quad (5.8)$$

According to (5.8), the factor f is determined by dividing the radiation increase $\Delta_{2 \times CO_2}^{(0)}$ resulting from CO_2 doubling at zero humidity by the surface temperature increase $\Delta T^{(H)}$ necessary for equilibrium of the earth's atmosphere for CO_2 doubling in the case of non-zero humidity.

Identifying $\Delta_{2 \times CO_2}^{(0)}/\Delta T^{(H)}$ in (5.8) with the experimentally measured slope $(\Delta Flux/\Delta T)_{exp}$ of the outgoing radiation at the TOA measured as a function of the sea-surface temperature,

$$\frac{\Delta_{2 \times CO_2}^{(0)}}{\Delta T^{(H)}} = \left(\frac{\Delta Flux}{\Delta T} \right)_{exp}, \quad (5.9)$$

we find that the factor f can be represented by

$$f \equiv f_{exp} = 1 - G(T) \left(\frac{\Delta Flux}{\Delta T} \right)_{exp}. \quad (5.10)$$

Relation (5.10) is due to Lindzen and Choi²⁰ § It allows one to deduce the climate sensitivity for non-zero humidity, $\Delta T^{(H)}$, see (5.5), from the experimentally determined radiation flux by inserting $f = f_{exp}$ according to (5.10), and the value of $\Delta T = \Delta T^{(0)} \simeq 1.1 K$ for CO_2 doubling at zero humidity.

Using satellite measurements of the ERBE¹⁵ and CERES¹⁶ collaborations, the detailed analysis in ref.²⁰ led to a value of

$$\left(\frac{\Delta Flux}{\Delta T} \right)_{exp} = 6.9 \pm 1.8 W m^{-2} K^{-1} \quad (5.11)$$

§ Compare equations (5) and (6) in ref.²⁰. Equation (6) contains an additional factor c via $f \rightarrow cf$ introduced for sharing of tropical feedbacks over the globe. The value of c depends on how the slope $\Delta Flux/\Delta T$ is extracted from measurements. A value of $c = 2$ is used in ref.²⁰. For a global value of $\Delta Flux/\Delta T$ one has $c \simeq 1$.

(see Table 2 in ref. ²⁰). Inserting this value into (5.10), we find

$$f_{exp} \cong 1 - 0.175 \times 6.9 \cong -0.21, \quad (5.12)$$

with $1 - f_{exp} \cong 1.21$, and $\Delta T^{(0)} \cong 1.07K$, from Table 8, from (5.5), we obtain

$$\Delta T_{exp} = \frac{1.07}{1.21} \simeq 0.9K. \quad (5.13)$$

Introducing the sharing factor $c = 2$ from ref. ²⁰, compare footnote g, we have $f_{exp} \cong -0.1$ and ΔT_{exp} becomes

$$\Delta T_{exp} = \frac{1.07}{1.1} \simeq 1.0K. \quad (5.14)$$

Lindzen and Choi, ²⁰, employing $c = 2$, find $f_{exp} = -0.5$ and consequently $\Delta T_{exp} \cong 0.7K$ (confidence interval $0.5K$ to $1.3K$ at 99 % confidence level).^h

In view of the complexity of the subject matter, we conclude that there is satisfactory agreement between the theoretical result of

$$\Delta T_{th} = 0.46K \simeq 0.5K \quad (5.15)$$

from Table 8,ⁱ and $T_{exp} \simeq 0.9K$ to $1.0K$ empirically obtained upon identifying the ratio of $\Delta_{2 \times CO_2}^{(0)}/\Delta T^{(H)}$ with the satellite-based radiation flux measurements, $\Delta Flux/\Delta T$. In fact, we conclude that the results from the satellite-based radiation-flux measurement support the results on the climate sensitivity from the detailed and reliable radiation-transfer calculations.

As pointed out in refs. ¹⁴ and ²⁰, there is definite disagreement between the results from the radiation-flux measurements of $f_{exp} < 0$, and the predictions of a large number of atmospheric models that arrive at a positive feedback factor $f > 0$ and an enhanced value of the climate sensitivity of $\Delta T(\text{atm. models}) \gg 1K$.

We add a reference to a recent paper ²² that responds to the claim ¹¹ of empirical support for a significant climate sensitivity, $\Delta T \gg 1K$, due to CO_2 doubling, based on the analysis of the observed changes of ΔT in the 25-year period from 1983 to 2008. It is pointed out ²² that the climate models employed ¹¹ for this analysis fail to correctly incorporate the important influence of the low-cloud-cover contribution on ΔT in the period under investigation. Correctly incorporating the cloud cover effect yields consistency with $\Delta T < 1K$ ²² in disagreement with the results of $\Delta T \gg 1K$ ¹¹.

^hThe difference between our result of $f_{exp} = -0.1$ for $c = 2$ and $\Delta T_{exp} \simeq 1K$, and the result from ref. ²⁰, namely $f_{exp} \simeq -0.5$ for $c = 2$ and $\Delta T_{exp} \simeq 0.7K$, is due to the difference between our value of $G = G(T = 293K) \cong 0.175KW^{-1}m^2$ and $G(T = 255K) \cong 0.3$ used in ref. ²⁰, or, equivalently $C_{2 \times CO_2}^{(0)} = 6.09Wm^{-2}$ versus $C_{2 \times CO_2}^{(0)} = \Delta Q = 3.7Wm^{-2}$ implying $T^{(0)} \simeq 1.1K$ in both cases.

ⁱCompare also the variation of the theoretical results in Table 9 under various atmospheric conditions.

6. Conclusions

It has been the aim of this paper to estimate the increase in temperature ΔT (“climate sensitivity”) of the surface of the earth due to a doubling of the CO_2 concentration in the atmosphere. The estimate is obtained in a concise and transparent manner without oversimplification. All necessary steps are explicitly elaborated upon.

The basic assumption of associating a uniform constant temperature T with the surface of the earth, and a black-body long-wave infrared radiation $S(T)$, is by no means trivial, implicitly or explicitly, however, common to main-stream investigations on this matter. Our results are based on a new radiative-transfer evaluation, the details being presented in Appendix A. The absorption of the atmosphere in the CO_2 spectral range can be, and is reliably determined, and leads to an approximately constant value beyond an altitude of about 5 km, or a length of the horizontal CO_2 -air pipe of about 3 km at surface temperature and pressure.

Assuming restoration of equilibrium upon doubling of the CO_2 concentration by an associated increase of the temperature then implies a definite estimate of the increase of the surface temperature ΔT , given by $\Delta T \cong 0.5 \text{ } ^\circ C$ (compare Sections 3 and 4).

In terms of the widely employed feedback parameter f , the result of $\Delta T \cong 0.5 \text{ } ^\circ C$ corresponds to a negative feedback of $f < 0$. This result is empirically supported by satellite-based measurements of short-time fluctuations of the outgoing radiation flux at the TOA as a function of (sea-)surface temperature. A consistent picture emerges by combining theoretical radiation-transfer results with radiation-flux measurements (compare Section 5). This picture disagrees with an abundant number of predictions from climate models that imply positive feedbacks, $f > 0$.

The quantitative result of $\Delta T \simeq 0.5$ to $0.6 \text{ } ^\circ C$ valid for the drastic increase of doubling of the CO_2 content in air from 380 ppm to 760 ppm to be related to one century, confirms that the effect of an anthropogenic CO_2 increase on the climate on earth is fairly negligible. This conclusion is in strong contrast to the values of $\Delta T \sim 1.5 - 4.5 \text{ } ^\circ C$ quoted in the 2013 IPCC report¹¹. The published results on ΔT fill an even larger interval between $\Delta T \simeq 0.4 \text{ } ^\circ C$ to $\Delta T \simeq 8 \text{ } ^\circ C$. There is a systematic tendency of the results on ΔT published between the years 2000 to 2018 to decrease¹² with increasing publication date, the results coming closer to our result of $\Delta T \simeq 0.5 \text{ } ^\circ C$.^j

We found a concise and brief derivation of the earth’s greenhouse effect (compare Appendix B, in particular Fig. B1). The greenhouse effect is explicitly derived. It is understood as a shift of the radiative equilibrium from the earth’s surface to an atmospheric level above approximately five kilometers.

^jCompare e.g. Fig. 1 in ref. ¹² and the associated list of tens of references.

Acknowledgements

The author thanks Konrad Kleinknecht for discussions that initiated the present investigation. The author thanks Peng-Sheng Wei for a useful correspondence. Particular thanks go to Roy Clark for providing the radiative transfer results in Appendix A, for much help in tracing the relevant literature on the subject matter, as well as a critical reading of the present paper.

Appendix A. CO_2 Absorbance 568 to 770 cm^{-1} , 7 km path, 296 K , 300 , 600 ppm

The configurations used for the pipe and atmospheric absorption calculations are shown in Figures A1a and A1b.

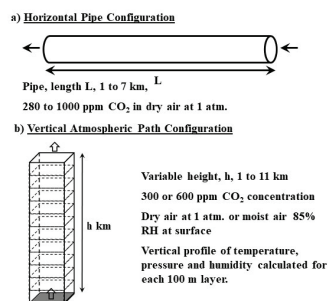


Fig. A1. Configurations used for the pipe and atmospheric absorption calculations.

For the ‘pipe’ configuration, a variable horizontal path length L , from 1 to 7 km long was used. The CO_2 concentration was varied from 280 to 1000 ppm. A total pressure of 1 atmosphere dry air at 293 K was used.

For the atmospheric absorption calculation, a vertical path, h , from 1 to 11 km was used. The surface temperature was set to 293 K at 1 atmosphere pressure. Two sets of calculations were performed. The first used dry air with a lapse rate of -6.5 K km^{-1} . The second used a surface relative humidity of 85 % with a lapse rate of -6.5 K km^{-1} up to the saturation level. Above the saturation level, the meteorological formula for the saturated lapse rate is used²³. The lapse rates used are plotted below in Fig. A6. The vertical atmospheric profile was calculated using a spatial resolution of 100 m.

The high resolution CO_2 absorbance spectra were calculated using spectral data from the HITRAN database⁵, $^{12}C^{16}O_2$ lines only with linestrengths $> 1e-23$. The spectral resolution was 0.01 cm^{-1} . The temperature was set to 293 K. For the ‘pipe’ calculations, the large spectral data files were divided into seven spectral ranges with the absorption coefficient calculated for each spectral range. The calculations were performed using Excel workbooks with each spectral range in a separate workbook. The weighted averages over the spectral ranges 568 to 770 cm^{-1} and 600 to 750 cm^{-1} were then calculated. The ‘pipe’ calculation is illustrated in Table A1. Path lengths of 1, 2, 3, 5 and 7 km were used. The results are given in Tables A2 and A3. Plots of the data are shown in Figures A2 and A3.

Table A1. The weighted averages of the seven spectral ranges are combined to give the band average absorption. R. Clark, April 28th 2019

Range cm^{-1}	Start/End	300 ppm	600 ppm
32	568 to 600 cm^{-1}	0.51	0.64
20	600 to 620 cm^{-1}	0.94	0.99
20	620 to 640 cm^{-1}	0.99	1.00
60	640 to 700 cm^{-1}	1.00	1.00
25	700 to 725 cm^{-1}	0.99	1.00
25	725 to 750 cm^{-1}	0.89	0.97
20	750 to 770 cm^{-1}	0.39	0.53
Band Average			
202	568 to 770 cm^{-1}	0.84	0.89
Absn coeff $-\ln(1-A)$		1.83	2.21
a ($\text{atm}^{-1} \text{m}^{-1}$)		0.870	0.527

Table A2. ‘Pipe’ absorption for selected path lengths from 1 to 7 km, CO_2 concentrations of 280 to 1000 ppm, 568 to 769 cm^{-1} spectral range, 293 K.

ppm	280	300	380	400	600	760	1000
1 km	0.62	0.63	0.66	0.66	0.71	0.73	0.76
2 km	0.70	0.71	0.73	0.74	0.78	0.81	0.83
3 km	0.75	0.75	0.78	0.78	0.82	0.84	0.87
5 km	0.80	0.81	0.83	0.83	0.87	0.88	0.90
7 km	0.83	0.84	0.86	0.86	0.89	0.90	0.92

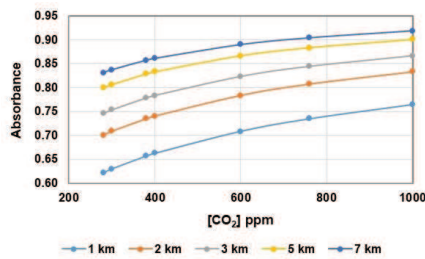


Fig. A2. Data plotted from Table A2.

Table A3. ‘Pipe’ Absorption for selected path lengths and concentrations, 1 to 7 km and 280 to 1000 ppm, 600 to 750 cm^{-1} spectral range

ppm	280	300	380	400	600	760	1000
1 km	0.78	0.79	0.82	0.83	0.87	0.89	0.92
2 km	0.86	0.87	0.89	0.90	0.93	0.95	0.97
3 km	0.90	0.91	0.93	0.93	0.96	0.97	0.98
5 km	0.94	0.95	0.96	0.97	0.98	0.99	0.99
7 km	0.96	0.97	0.98	0.98	0.99	1.00	1.00

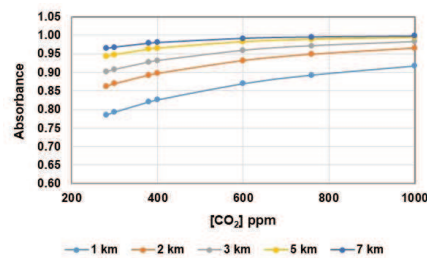


Fig. A3. Data plotted from Table A3.

The atmospheric radiative transfer calculations were performed using the same CO_2 lines that were used for the ‘pipe’ calculations with $^1\text{H}_2^{16}\text{O}$ lines with linestrengths $> 1\text{e-}23$ added for the 85 % RH cases. The calculations were performed using Excel VBA macros at a spectral resolution of 0.01 cm^{-1} . However, the data were binned into 1 cm^{-1} intervals for plotting. The conditions of temperature and CO_2 concentration and the spectral ranges were the same as for the ‘pipe’ data. The H_2O concentration was set to a relative humidity of 85 % at 293 K for the first 100 m layer. The vertical path length was varied from 1 to 11 km in 1 km steps. The results are given in Tables A4 and A5. Plots of the data are shown in Figures A4 and A5.

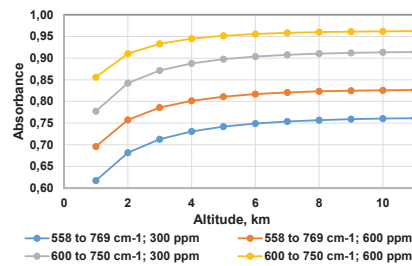


Fig. A4. Data plotted from Table A4.

Table A4. Atmospheric absorption data for the spectral range from 568 to 769 cm^{-1} and from 600 to 750 cm^{-1} . The vertical heights from the surface were varied from 1 to 11 km.

Altitude km	568 to 769 cm^{-1}		600 to 750 cm^{-1}	
	300 ppm	600 ppm	300 ppm	600 ppm
1	0.618	0.696	0.777	0.856
2	0.682	0.758	0.842	0.910
3	0.713	0.786	0.872	0.933
4	0.731	0.802	0.888	0.945
5	0.742	0.811	0.897	0.952
6	0.749	0.817	0.904	0.956
7	0.754	0.821	0.908	0.958
8	0.757	0.823	0.910	0.960
9	0.759	0.825	0.912	0.961
10	0.761	0.826	0.913	0.962
11	0.761	0.827	0.914	0.962

Table A5. Atmospheric absorption data for the spectral range from 558 to 769 cm^{-1} and from 600 to 750 cm^{-1} . The vertical heights from the surface were varied from 1 to 11 km.

Altitude km	558 to 769 cm^{-1}		600 to 750 cm^{-1}	
	300 ppm, 85 RH	600 ppm, 85 RH	300 ppm, 85 RH	600 ppm, 85 RH
1	0.799	0.843	0.856	0.904
2	0.854	0.892	0.906	0.945
3	0.876	0.910	0.927	0.961
4	0.887	0.919	0.937	0.968
5	0.894	0.924	0.943	0.973
6	0.897	0.927	0.947	0.975
7	0.900	0.929	0.949	0.977
8	0.901	0.930	0.951	0.977
9	0.902	0.931	0.952	0.978
10	0.903	0.931	0.952	0.978
11	0.903	0.929	0.953	0.977

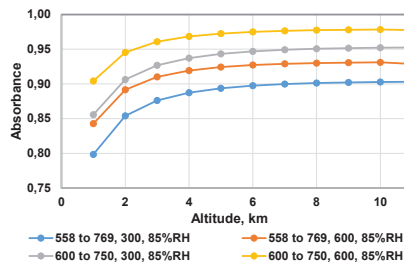


Fig. A5. Data plotted from Table A5.

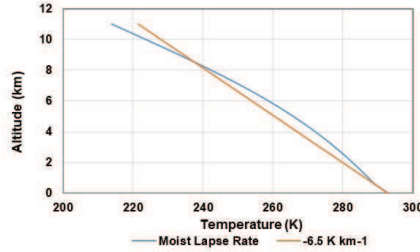


Fig. A6. The lapse rates used in the atmospheric absorption calculations, from ²³.

Appendix B. A Concise Representation of the Radiative “Greenhouse Effect” in the Atmosphere

The surface of the earth receives a net radiation from the sun, S_0 , of approximately $S_0 \simeq 240 \text{ W m}^{-2}$, see footnote b in the main text. The infrared radiation from the surface of the earth, the LWIR, contains a component, S_W , restricted in its spectral range to the so-called “atmospheric window”, and a second component, S_{up} . The second component consists of a small part, $f' S_{up}$ ($f' \ll 1$), emitted to space, and a larger fraction, $(1 - f') S_{up}$ that is absorbed by the so-called “greenhouse gases”, essentially H_2O and CO_2 , in the atmosphere, and subsequently re-emitted, partly to space, A_{up} , and partly down to the surface, A_{down} , compare Fig. B1.

The “transmittance parameter” f' , with $0 \leq f' \leq 1$, realistic values being restricted to $f' \ll 1$, quantifies the transmittance of the earth’s surface radiation in the spectral range outside the atmospheric window. Compare the incomplete saturation of the absorption in Fig. 4a at altitudes larger than (approximately) 9 km.

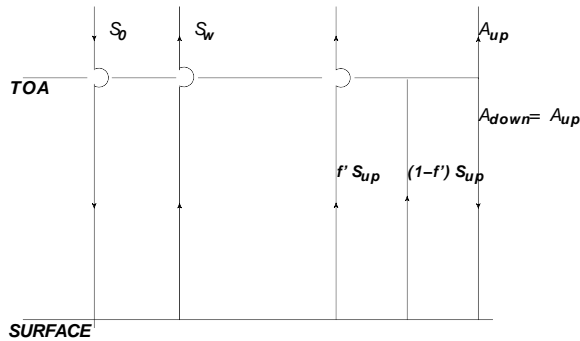


Fig. B1. Schematic representation of the net radiation from the sun, $S_0 \simeq 240 \text{ W m}^{-2}$, the infrared radiation to space through the atmospheric window, S_W , the infrared radiation from the surface to space $f' S_{up}$, and to the atmosphere $(1 - f') S_{up}$, where $f' \ll 1$, and the radiation from the atmosphere to space A_{up} and to the surface, A_{down} .

Global radiative equilibrium of the earth is due to an equality between the intensity of the short-wave radiation received from the sun, S_0 , and the infrared radiation sent out to space, i.e.

$$S_0 = S_W + f' S_{up} + A_{up}. \quad (\text{B.1})$$

Equilibrium at the upper atmosphere (the top of the atmosphere, TOA) requires

$$(1 - f') S_{up} = A_{up} + A_{down} = 2A_{up}, \quad (\text{B.2})$$

where equality of the upward and the downward emission from the greenhouse gases has been employed in the second step. From (B.1) and (B.2), we deduce the radiation from the surface, S_{up} , given by

$$S_{up} = \frac{2}{1 + f'} (S_0 - S_W), \quad (\text{B.3})$$

as well as the radiation from the TOA,

$$A_{up} = A_{down} = \frac{1 - f'}{1 + f'} (S_0 - S_W). \quad (\text{B.4})$$

Both, S_{up} and A_{up} are expressed in terms of $S_0 - S_W$, that is the radiation from the sun upon reduction by the radiation, S_W , that is associated with the transmission of radiation through the atmospheric window.

For given S_0 , from (B.3), we find that the total emission by the surface, $S_{tot,surf}(S_W, f')$, is given by

$$S_{tot,surf}(S_W, f') = S_W + S_{up} = S_0 \left(\frac{2}{1 + f'} - \frac{S_W}{S_0} \frac{1 - f'}{1 + f'} \right) \equiv S_0 c \left(\frac{S_W}{S_0}, f' \right). \quad (\text{B.5})$$

Employing (B.3) and (B.4), one may explicitly check the validity of equilibrium at the surface,

$$S_{tot,surf} = S_W + S_{up} = S_0 + A_{down} = S_0 + A_{up}. \quad (\text{B.6})$$

The radiation to space at the TOA,

$$S_{tot,TOA}(S_W, f') = S_W + f' S_{up} + A_{up}, \quad (\text{B.7})$$

upon substitution of the results for S_{up} and for A_{up} from (B.3) and (B.4) becomes

$$S_{tot,TOA}(S_W, f') = S_0. \quad (\text{B.8})$$

Global radiative equilibrium (B.1) is realized by the equality of the radiation intensities emitted from the TOA, $S_{tot,TOA}$, and received from the sun, S_0 .

It will be illuminating to numerically evaluate our main result, the expression for the surface radiation (B.5), for several relevant values of S_W and f' for fixed $S_0 = 240 \text{ W m}^{-2}$.

Upon assuming a Planck black-body radiation spectrum for the surface radiation (B.5),

$$S_{tot,surf}(S_W, f') = \sigma (T_{surf}(S_W, f'))^4, \quad (\text{B.9})$$

where $\sigma \cong 5.670 \times 10^{-8} W m^{-2} K^{-4}$, we obtain the associated surface temperature,

$$\begin{aligned} T_{surf}(S_W, f') &= \left(\frac{S_0}{\sigma}\right)^{\frac{1}{4}} \left(\frac{2}{1+f'} - \frac{S_W}{S_0} \frac{1-f'}{1+f'}\right)^{\frac{1}{4}} \\ &= 255.069 \left(\frac{2}{1+f'} - \frac{S_W}{S_0} \frac{1-f'}{1+f'}\right)^{\frac{1}{4}} K \\ &= 255.069 c \left(\frac{S_W}{S_0}, f'\right)^{\frac{1}{4}} K. \end{aligned} \quad (B.10)$$

Relations (B.5) and (B.10) give the equilibrium surface radiation and surface temperature for given values of S_0 , S_W and f' .

The numerical results for $S_{tot, surf}$ from (B.5) and T_{surf} from (B.10) for a few representative values of S_W are collected in Table B1.

Table B1. Numerical results for the total surface radiation $S_{tot, surf}(S_W, f')$ given by (B.5), and for the surface temperature $T_{surf}(S_W, f')$ given by (B.10).

$S_W [W m^{-2}](f')$	$c \left(\frac{S_W}{S_0}, f'\right)$	$S_{tot, surf} [W m^{-2}]$	$T_{surf} [K]$
240 and/or $f' = 1$	1.0	240	$255 = -18^0 \text{ C}$
58 ($f' = 0.1$)	1.62	389	$288 = 15^0 \text{ C}$
43 ($f' = 0.1$)	1.67	401	$290 = 17^0 \text{ C}$
28 ($f' = 0.1$)	1.72	413	$292 = 19^0 \text{ C}$
0 ($f' = 0.1$)	1.82	436	$296 = 23^0 \text{ C}$
0 ($f' = 0$)	2.0	480	$303 = 30^0 \text{ C}$

Turning to a discussion of the results in Table B1, we start with the results for the empirical input of $S_W = 43 \pm 15 W m^{-2}$, or $58 \geq S_W \geq 28 W m^{-2}$, deduced⁸ from meteorological measurements of the long-wave infrared radiation (LWIR). The value of $f' = 0.1$ follows from Table 6 in the main text. At the saturation limit (for $C O_2$ content of 300 ppm) the absorption reaches a value of $A = 0.90$. This corresponds to $(1 - f')S_{up} = 0.90S_{up}$, or $f' = 0.1$. The results for the surface temperature, T_{surf} , from (B.10) given by $288 \leq T_{surf} \leq 292 K$, or 15^0 C to 19^0 C , are consistent with the very elaborate theoretical analysis in refs.⁴ and¹⁰.

The case of $S_W = S_0 = 240 W m^{-2}$ in the first line of Table B1, according to (B.3) and (B.4), corresponds to $S_{up} = A_{up} = 0$. This is the hypothetical case of an atmosphere allowing for direct total emission from the surface to space, or zero absorption, no greenhouse gas present. Comparing $S_{tot surf}(S_W = S_0, f')$ with (B.8), we find the identity

$$S_{tot TOA}(S_W, f') = S_{tot surf}(S_W = S_0, f'). \quad (B.11)$$

The infrared radiation at the TOA, $S_{tot\ TOA}(S_W, f') = S_0$, is equal to the surface radiation of a non-absorbing hypothetical atmosphere^k. The associated temperature is given by $T_{TOA} = T_{surf} = 255K$. The “greenhouse effect” of the atmosphere containing “greenhouse gases” consists of shifting the origin of the outgoing infrared radiation (responsible for equilibrium with the radiation from the sun) from the surface to the TOA.

The hypothetical limit of $S_W = 0$ and $f' = 0$ in the last line of Table B1 describes the case of a hypothetical “closed atmospheric window”, total absorption of the emitted surface radiation of $S_{tot, surf}(S_W = 0, f' = 0) = 2S_0$, implying the maximally possible equilibrium surface temperature of $T_{surf} = 303K = 30^0C$.

A comment on the consistency of our results with the radiation and energy budget analysis in ref.⁴ is appropriate. Trenberth et al.⁴, using $S'_0 = 239Wm^{-2}$ as input solar radiation, find a total surface radiation, $S'_{tot\ surf} = 396Wm^{-2}$ corresponding to $T' = 289K = 16^0C$, consistent with our result from Table B1, $S_{tot\ surf} \simeq 401Wm^{-2}$ and $T = 17^0C$. The consistency is not accidental, but can be understood as follows.

According to ref.⁴, in our notation, the downward radiation is given by $A'_{down} = 333Wm^{-2}$. Including the amount of $78Wm^{-2}$ of solar radiation absorbed by the atmosphere into the solar radiation absorbed by the surface, one effectively has $A''_{down} = 333 - 78 = 255Wm^{-2}$. Thermals and evaporation amount to $97Wm^{-2}$. From our point of view they should be considered as being independent from the radiation budget. The amount of $97Wm^{-2}$ quantifies the energy conversion of an adiabatic heat engine working between the temperatures of $T = 289K$ on the surface, and $T = 255K$ at the TOA. The heat engine, working in the gravitational field of the earth, solely continuously converts internal energy of the air at $T = 289K$ back and forth into potential energy at $T = 255K$. This process does not affect the radiative balance, and accordingly, $A'_{down} = 333Wm^{-2}$ is reduced to $A'''_{down} = 333 - 78 - 97 = 158Wm^{-2}$, a value consistent with $A_{down} = 161Wm^{-2}$ from (B.4).

The radiation balance obtained by Trenberth et al.⁴ accordingly is consistently reduced to the simple representation shown in Fig. C1 that contains the essential features of the greenhouse effect.

We turn to the change of the surface radiation under doubling of the atmospheric CO_2 content, and the associated change of the surface temperature ΔT discussed in section 3 of the main text.

For a small change of the parameter $f' \rightarrow f' + \Delta f'$, with $S_W = const$, from (B.5) and (B.6) we find

$$\frac{dS_{up}(S_W, f')}{df'} = \frac{dS_{tot, surf}(S_W, f')}{df'} = -\frac{2(S_0 - S_W)}{(1 + f')^2}, \quad (B.12)$$

^kEquivalently, the non-absorbing atmosphere may be described by inserting $f' = 1$ in (B.5), implying $S_{tot\ surf}(S_W, f' = 1) = S_0$ and $A_{up} = A_{down} = 0$ according to (B.4).

or

$$\Delta f' = -\frac{(1+f')^2}{2(S_0 - S_W)} \Delta S_{up} = -\frac{(1+f')^2}{2(S_0 - S_W)} \Delta_{2 \times CO_2}, \quad (\text{B.13})$$

where $\Delta S_{up} = \Delta S_{tot, surf} = \Delta_{2 \times CO_2}$, due to CO_2 doubling, was inserted in the second step. The negative value of $\Delta f' < 0$ for $\Delta_{2 \times CO_2} > 0$ implies less direct radiation to space and, accordingly, a rise of the surface temperature, $\Delta T > 0$.

For the change of the surface temperature T_{surf} , from (B.10), we obtain

$$\Delta T = \frac{dT}{df'} df' = -\frac{T_{surf}}{4} \frac{2 \left(1 - \frac{S_W}{S_0}\right)}{2(1+f') - \frac{S_W}{S_0}(1-f'^2)} \Delta f' = \frac{T_{surf}}{4} \frac{\Delta_{2 \times CO_2}}{S_{tot, surf}(S_W, f')}, \quad (\text{B.14})$$

where $\Delta f'$ from (B.13) was inserted in the last step. The expression resulting from the insertion was simplified to yield the expression for $S_{tot, surf}(S_W, f')$ in (B.5) in the denominator of (B.14).

The agreement of ΔT in (B.14) with ΔT in (3.3) of the main text comes without surprise. We note however, that the present derivation of (B.14), relying on (B.5) and (B.10), assures equilibrium of radiation at the earth's surface and at the TOA for any given values of S_0, S_W, f' , and for $f' \rightarrow f' + \Delta f'$ in particular. In slight distinction from the present derivation of (B.14), in (3.3), we relied on using restoration of equilibrium upon CO_2 doubling. It is noteworthy, moreover, that T_{surf} in (B.10) and ΔT in (B.14) is predicted from the empirically known values of S_0, S_W and f' , while T_{surf} in (3.3) was used as an input parameter.

Table B2. Numerical results for the total surface radiation $S_{tot, surf}(S_W, f')$ according to (B.5), and the surface temperature, given by (B.10), as well as the temperature difference consistently also obtained from (B.14).

$S_W [Wm^{-2}](f')$	$c \left(\frac{S_W}{S_0}, f'\right)$	$S_{tot, surf} [Wm^{-2}]$	$T_{surf} [K]$
43	1.67159	401.182	290.028
($f' = 0.100$)			
43	1.68250	403.800	290.500
($f' = 0.092015$)			
		$\Delta S_{up} = \Delta_{2 \times CO_2} = 2.6$	$\Delta T = 0.47$

The numerical results in Table B2 are based on the input parameters, $S_0 = 240 Wm^{-2}$ and $S_W = 43 Wm^{-2}$, as well as $f' = 0.1$ and $f' = 0.1 + \Delta f' = 0.092015$, as obtained by evaluation of (B.13) for $\Delta_{2 \times CO_2} = 2.6 Wm^{-2}$ taken from Table 6.

In a first step, upon evaluating (B.5) and (B.10), we obtained the surface radiation and surface temperature shown in the second and third lines of Table B2. The subtraction of the two surface temperatures from each other then yields $\Delta T = 0.47 K$ shown in the last line of Table B2. In a second step, we confirm

$\Delta T = 0.47K$ ¹ by evaluating (B.14) by either inserting $\Delta f'$ from (B.13) or by directly inserting $\Delta_{2\times CO_2} = 2.6Wm^{-2}$.

References

1. A. Schack, *Phys. Blätter* **28** 26 (1972).
2. A. Schack, *Der industrielle Wärmeübergang* (Verlag Stahleisen m.b.H. Düsseldorf, 1. Auflage 1929, 8. Auflage 1983).
3. F. Gervais, *Internat. Journal of Mod. Phys. B* **28**, 1450095 (2014);
F. Gervais, *L'urgence climatique est un leurre* (Editions de l'Artilleur, 75008 Paris, 2018).
4. K.E. Trenberth, J.T. Fasullo and J. Kiehl, *Bull. Am. Meteorol. Soc.* **90** 311 (2009).
5. HITRAN data base.
6. Peng-Shen Wei et al., *Heliyon* **4**, e00785 (2018).
7. R. Clark, Ventura Photonics, private communication, see Appendix A.
8. R. Clark, *Energy and Environment* **24**, 319 and 341 (2013), Ventura Photonics Monograph VPM 005 (2019).
9. G.V. Chilingir et al., *Atmospheric and Climate Sciences* **4**, 819 (2014);
O.G. Sorokhatin et al., *Global Warming and Global Cooling: Evolution of Climate on Earth* (Elsevier 2007).
10. H. Harde, *Internat. Journal of Atmospheric Sciences* **2017**, Article ID 9251034.
11. *Fifth Assessment Report of the Intergovernmental Panel on Climate Change (IPCC), AR5*, ed. T.F. Stocker et al., Climate Change 2013; The Physical Science Basis, (Cambridge University Press, New York, NY, USA, 2014).
12. F. Gervais, *Earth Sciences Reviews* **155**, 129 (2016).
13. R.S. Lindzen, M.-D. Chou and A.Y. Hou, *Bull. Am. Meteorol. Soc.* **82**, 417 (2001).
14. R.S. Lindzen and Y.-S. Choi, *Geophys. Res. Lett.* **36**, L16705 (2009).
15. B.R. Barkstrom, *Bull. Am. Meteorol. Soc.* **65**, 1170 (1984).
16. B.A. Wielicki et al., *IEEE Trans. Geosci. Remote Sens.* **36**, 1127-1141 (1998).
17. E.-S. Chung, B.J. Soden, B.-J. Sohn, *Geophys. Res. Lett.* **37**, L10703 (2010).
18. D.M. Murphy et al., *Geophys. Res. Lett.* **37**, L09704 (2010).
19. K.E. Trenberth, J.T. Fasullo, C. O'Dell and T. Wong, *Geophys. Res. Lett.* **37**, L03702 (2010).
20. R.S. Lindzen and Y.-S. Choi, *Asia-Pacific J. Atmos. Sci.* **47** (4), 377 (2011).
21. J.R. Bates, *Earth and Space Science* **3**, 207 (2016).
22. J. Kauppinen and P. Malmi, "No experimental evidence for the significant anthropogenic climate change", arXiv: 1907.00165v1 [physics.ao-ph].
23. A. A. Tsonis, *Atmospheric Thermodynamics*, (2nd Edition, Cambridge University Press, Cambridge UK, 2007).

¹The discrepancy between $\Delta T = 0.47K$ in Table B2 and $\Delta T = 0.46K$ in Table 8 of the main text is due to the different input of $T = 293K$ in the main text.